A Numerical Investigation of the Dynamic Behaviour of Functionally Graded Foams

Stephen Kiernan, Liang Cui and Michael. D. Gilchrist

Abstract Two Finite Element models approximating the dynamic behaviour of functionally graded foam materials (FGFMs) have been developed under free weight drop impact and Kolsky wave propagation conditions. The FGFM is modeled by discretising the material into a large number of layers through the foam thickness. Each layer is described by a unique constitutive cellular response, which is derived from the initial relative density, ρ^*, unique to that layer. Large strain unixial compressive tests at strain rates of 0.001, 0.01 and 0.1/s were performed on expanded polystyrene (EPS) and ALPORAS® Aluminium (Al) foam and their $\sigma - \varepsilon$ response was used as input to a modified constitutive model from the literature. Simulations were then performed on both uniform and graded specimens. For both impact and wave propagation conditions it is found that under certain conditions an FGFM can outperform a uniform foam of equivalent density in terms of reducing peak accelerations imparted from an impact, or mitigating stress wave magnitudes through increased plastic deformation. These properties provide significant insight into the hypothesised behaviour of FGFMs and elucidate the potential for the future use in the design of next generation cushioning structures.

Stephen Kiernan
School of Electrical, Electronic & Mechanical Engineering, University College Dublin, e-mail: stephen.kiernan@ucd.ie

Liang Cui
School of Electrical, Electronic & Mechanical Engineering, University College Dublin e-mail: liang.cui@ucd.ie

Michael D. Gilchrist
School of Electrical, Electronic & Mechanical Engineering, University College Dublin michael.gilchrist@ucd.ie

1 Introduction

Cellular foams are widely used in energy absorbing applications where it is important to minimise the peak acceleration of the impacting body [1], e.g packaging of fragile goods, protective headgear [2, 3] and body garments. This is due to their low volume fraction of solid material and their complex microstructure which allows large degrees of plastic crushing to occur at a fairly constant plateau stress value. This plastic crushing at a constant stress will continue until, depending on the initial density, a densification strain is reached when cell walls and struts impinge on one another and further crushing is of the material matrix itself rather than the foam cells. Understanding their dynamic stress-strain behaviour at finite deformations is therefore essential in order to predict their performance as cushioning materials.

The compressive static and impact loading response of polymeric foams has been previously characterised [4] using energy absorption and efficiency diagrams. They showed that, for a particular density, a foam is most efficient at absorbing the kinetic energy, KE, of an impact over a limited range of stress; if the imparted stress is too little the foam will not yield, too great and the foam will densify and become much like a solid. It is hypothesised that by means of a functionally graded foam, it may be possible to incorporate a continuously varying density in either one, two, or three dimensions to improve the energy absorbing efficiency over a wider range of stress.

The Split Hopkinson Pressure Bar technique has proved to be extremely versatile in material characterization and has grown from its original configuration for compression testing to include tension, torsion and fracture testing [5]. It has been used to characterise the dynamic response of a multitude of materials such as soils [6], composites [7], and metals [8]. Foams have also been studied using the SHPB technique [9]. From 1-D elastic wave theory, $\sigma_s(t)$, $\varepsilon_s(t)$, and $\dot{\varepsilon}_s(t)$ of a SHPB specimen are obtained from the transmitted, (ε_T), and reflected, (ε_R), found from the induced strain pulses measured in the apparatus bars from the equations:

$$\dot{\varepsilon}_s(t) = -\frac{2C_0}{L_s}\varepsilon_\mathrm{R}(t) \tag{1}$$

$$\varepsilon_s(t) = -\frac{2C_0}{L_s}\int_0^t \varepsilon_\mathrm{R}(t)dt \tag{2}$$

$$\sigma_s(t) = E_b\frac{A_b}{A_s}\varepsilon_\mathrm{T}(t) \tag{3}$$

where $\dot{\varepsilon}_s(t)$, $\varepsilon_s(t)$, $\sigma_s(t)$ are strain rate, strain and stress respectively. C_0 is the wave speed within the bar, L_s is the length or thickness of the specimen, A_s and A_b are the cross-sectional area of the specimen and the bar, respectively, and E_b is Young's modulus of the bar.

Nature has employed Functionally Graded Materials (FGMs) to optimise weight to strength ratios in response to non-uniform load distributions (e.g. cortical / trabecular bone, bamboo) and ensure no peak stresses occur at any point in the structure [10]. This is an adaptive process, evolving over time, but increasingly designers are

investigating methods of optimising structures through gradient material properties. The current study aims to design a virtual, novel FGFM which contains micro-scale cells varied continuously in a predefined manner for the purpose of improving its energy absorbing characteristics under physical impact and wave propagation conditions.

This paper first describes the methodology of obtaining the multiple $\sigma - \varepsilon$ curves required to describe the FGFM. Sections 2.1 and 2.2 then briefly detail the models used to approximate an FGFM under striker impact and Kolsky wave conditions respectively, along with the indicative results. Section 3 discusses these results with respect to improved energy management[1]. Finally, Section 3.3 presents the important conclusions from this work.

2 Methodology

Large strain uniaxial compressive tests at strain rates of 0.001, 0.01 and 0.1/s were performed on five EPS foams with densities of 15, 20, 25, 50, and 64kg/m^3, and one ALPORAS® Al foam of density $\approx$ 250kg/m^3 to determine their $\sigma - \varepsilon$ response - compressive curves are required as input to the ABAQUS [11] crushable foam model used in this work. Obtaining complete experimental $\sigma - \varepsilon$ curves for the many layers required in each model (up to 50 layers) was impractical so a FORTRAN program, incorporating an existing model from the literature that describes the uniaxial compressive behaviour of uniform foam [12], was written. Experimental data was used to calibrate the program's output, and based on the empirical observation that a foam's ρ^* largely dictates its compressive $\sigma - \varepsilon$ behavior, arbitrary $\sigma - \varepsilon$ curves could be generated through interpolation and extrapolation of ρ^* from the available experimental data. The curves generated by this program were validated against the $\sigma - \varepsilon$ curves of the EPS and ALPORAS® physical compression tests. By applying a unique $\sigma - \varepsilon$ definition to each layer using the ABAQUS crushable foam model, a quasi-graded (see Table 1) cellular material could them be virtually created. All simulations were carried out using reduced integration, 3-D, 8-node hexahedral elements with hourglass control, as an explicit dynamic analysis and solved using an explicit central difference integration rule. Strain rate effects are not considered within the scope of this study.

2.1 Striker Impacts

Figure 1 illustrates the virtual test configuration and Table 1 shows the test parameters used in the physical impact simulations, and refers to a single striker mass and density range ($\Delta\rho$). Striker masses of 1, 2, 4, 6, 8, 10, 12 and 14kg were also

[1] reducing peak g, increasing stress energy mitigation

simulated, giving a total of 440 simulations to parametrically study the effect of the selected variables.

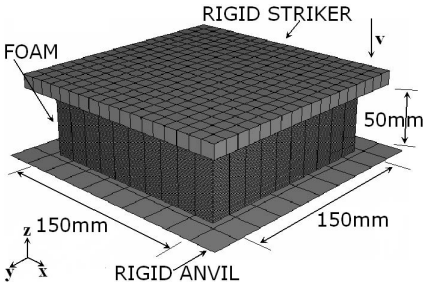

Figure 1 The foam is composed of 50 layers, each defined with a unique cellular response. In addition to uniform foam, five gradients were investigated (Table 1), which all monotonically decrease from the striker to anvil face. Preliminary simulations showed that monotonically decreasing the density from the striker to anvil face resulted in a decrease in peak g values[2]. The anvil is encastre constrained and the striker may only move in the Z-direction. A single impact velocity of 5.425m/s was chosen.

Table 1 Material gradients with density ranges used in striker impact simulations.

Gradients	Density Range[a] (kg/m^3) $\Delta\rho = 20$				
Uniform	44	54	64	84	104
Logarithmic	59.2 - 39.2	69.2 - 49.2	79.2 - 59.2	99.2 - 79.2	119.2 - 99.2
Square Root	57.3 - 37.3	67.3 - 47.3	77.3 - 57.3	97.3 - 77.3	117.3 - 97.3
Linear	54.0 - 34.0	66.0 - 44.0	74.0 - 54.0	94.0 - 74.0	114.0 - 94.0
Quadratic	50.8 - 30.8	60.8 - 40.8	70.8 - 50.8	90.8 - 70.8	110.8 - 90.8
Cubic	49.2 - 29.2	59.2 - 39.2	69.2 - 49.2	89.2 - 69.2	109.2 - 89.2
Gradients	Density Range[a] (kg/m^3) $\Delta\rho = 40$				
Uniform	44	54	64	84	104
Logarithmic	74.4 - 34.4	84.4 - 44.4	94.4 - 54.4	114.4 - 74.4	134.4 - 94.4
Square Root	70.6 - 30.6	80.6 - 40.6	90.6 - 50.6	110.6 - 70.6	130.6 - 90.6
Linear	64.0 - 24.0	74.0 - 34.0	84.0 - 44.0	104.0 - 64.0	124.0 - 84.0
Quadratic	57.5 - 17.5	67.5 - 27.5	77.5 - 37.5	97.5 - 57.5	117.5 - 77.5
Cubic	54.2 - 14.2	64.2 - 24.2	74.2 - 34.2	94.2 - 54.2	114.2 - 74.2

[a] Densities are derived from EPS compression tests.

2.2 Split Hopkinson Pressure Bar

A three dimensional model comprised of projectile, incident bar, specimen and transmission bar was created to simulate one dimensional wave propagation through

[2] Conversely, monotonically increasing the density from the striker to anvil face resulted in an increase in peak g values, relative to a uniform foam of equal ρ^*_{average}.

an FGFM specimen, the bar strains of which were validated against experiments carried out using a wide area SHPB apparatus. This ensures that valid boundary conditions are applied to the virtual FGFM specimens. The experimental transmission and incident bars were made from 30% glass filled nylon, to minimise impedance mismatch with the specimen, and were 1000mm long with a 50mm diameter. These were approximated as linear elastic during modeling. Projectile lengths of 150mm and 250mm were simulated at the same impact velocities used during the validation experiments; 19m/s and 13m/s respectively. A virtual specimen length of 300mm is used to illustrate the differing response between a uniform and a functionally graded foam. This methodology is sound because results are taken directly from the F.E. specimen rather than derived from the bar strains, thus negating the assumptions that Equations 1, 2 and 3 are derived from. During the validation experiments wave disperson was observed in the incident and transmission bars due to their viscoelastic nature and so wave corrections using Fourier Theory and following the works of [13] and [14] was carried out during post-processing to shift the incident and transmissions waves to the bar specimen interfaces. Table 2 shows the test parameters used in the simulations.

Table 2 Material gradients with density ranges used in SHPB simulations.

Gradients	Density Range[b] (kg/m^3)		
	$\Delta\rho$ = 100	$\Delta\rho$ = 50	$\Delta\rho$= 20
Uniform	250.0	250.0	250.0
Logarithmic	179.3 - 279.3	—	—
Square Root	184.4 - 284.4	—	—
Linear	200.0 - 300.0	225 - 275	240 - 260
Quadratic	215.8 - 315.8	—	—
Cubic	223.7 - 323.7	—	—

[b] Densities are derived from ALPORAS® compression tests.

3 Discussion

3.1 Striker Impacts

The shape of Figure 2 is indicative of an FGFMs impact response for the different average densities examined. For low kinetic energy impacts, the graded foam performs better[2] than the uniform foam (e.g. $\rho_{average}$ = 54 kg/m^3, mass = 1 kg) and the convex gradients (e.g. quadratic) perform better than the concave gradients (e.g. square root). However, as the impacting mass (and therefore KE) is increased to 14 kg, an opposite trend is observed (see Figure 2). The marked improvement of the

[2] greatly reduced peak accelerations relative to that of a uniform foam of equal $\rho_{average}$

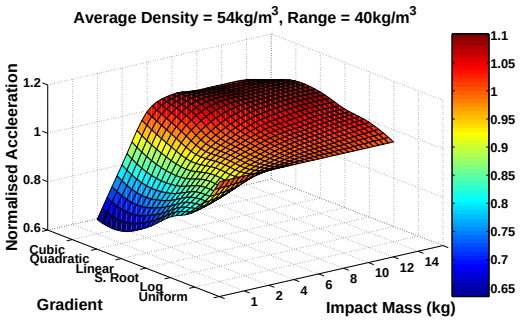

Figure 2 The influence of multiple input parameters (in this case impact mass and material gradient) on a desired output, such as peak acceleration can be clearly seen through the use of design surface plots. Acceleration has been normalised against the peak acceleration of the striker impacting a uniform foam of equal ρ^*_{average}

FGFM over the uniform foam in reducing the peak acceleration of the lower energy impacts can be explained as follows. It has been stated previously that foam with a single density is most efficient at absorbing energy when it works within the plateau strain region, up to densification, as it absorbs most energy under large plastic strains with little corresponding increase in stress. From simulation it was found that for a uniform foam of 44 kg/m^3, the stress imparted at the time of peak acceleration was 198 kPa for a striker mass of 1 kg and was 581 kPa for a striker mass of 14 kg. From the experimental $\sigma - \varepsilon$ compression tests and FORTRAN program (Sect. 2) it can be deduced that 44 kg/m^3 EPS foam will yield at about 310 kPa and thus will not yield when struck with a striker of 1 kg at 5.425m/s, but rather will behave elastically with very little deformation, resulting in high peak accelerations. However, when struck with a striker of 14 kg at 5.425m/s it will absorb the corresponding kinetic energy within the plateau stress region up to 0.6 strain. The FGFMs perform distinctly better than the uniform foam when absorbing the lower energies due to their spatially varying yield surface, a direct result of the density gradient. From Table 2, for example, the density of a quadratically varying foam with $\Delta\rho = 40\ kg/m^3$ will vary from 54.2 kg/m^3 to 14.2 kg/m^3. At 14.2 kg/m^3, local plastic deformation was found from simulations to initiate at about 100 kPa, deforming to almost 0.7 strain, and approximately 20% by volume (14.2 - 28 kg/m^3) of the graded foam will yield plastically at a stress of 198 kPa. This is in stark contrast to the equivalent uniform foam, which exhibits no yielding at this stress level. As the kinetic energy of the striker is increased the advantage gained by a varying yield surface diminishes rapidly. Low yielding regions of the FGFM are no longer effective and local deformation beyond their densification strains occurs while mitigating only a small fraction of the total energy. Results show that a uniform 44 kg/m^3 foam experiences 0.54 strain at the incident surface and 0.52 strain at the distal surface when impacted by a 14 kg striker at 5.425m/s. In contrast, the quadratically varying FGFM deforms locally to only 0.2 strain at the incident surface and yet there is 0.98 strain at the distal face. Intuitively, and from previous work [4], it is more advantageous for a foam's entire volume to deform up to, but not beyond, its densification strain if it is to act most effectively as a cushioning structure.

3.2 Split Hopkinson Pressure Bar

Figures 3(a) and 3(b) shows strain-time traces of the strain wave recorded in the virtual transmission bar for a uniform foam of density 250kg/m^3 and five gradiented foams for the cases of increasing and decreasing density in the direction of wave propagation respectively. Although Figure 3(a) shows logarithmic and square root functions to be slightly more efficient at reducing the amount of stress transmitted, Figure 3(b) highlights the importance of the orientation of the material gradient. The decrease in transmitted strain (and consequently stress) achieved by employing a gradient foam indicates that the specific stress absorbed (Pa.m^{-3}.kg^{-1}) by the gradient foam, from the incident wave, is increased.

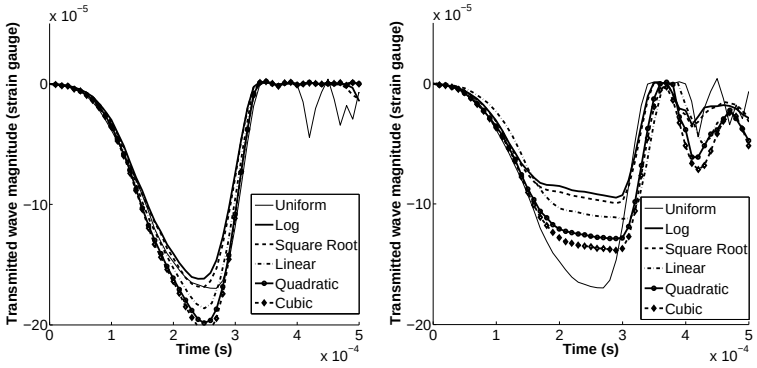

(a) Increasing density (b) Decreasing density

Figure 3 Comparison of transmitted wave as measured from the strain gauge for the uniform specimen and the FGFM specimens ($\Delta\rho$=100 kg/m^3)

The main mechanism by which a foam absorbs energy or attenuates stress is through plastic deformation. As the stress wave propagates along the *z*-direction through a uniform foam, it will plastically deform the foam until its magnitude σ_w becomes lower than the foam's yield stress σ_y. Once this occurs, the remainder of the wave will propagate elastically with little additional energy dissipated since no more plastic deformation will occur. It can be deduced that if σ_y were to decrease in the *z*-direction there would be a time delay in σ_w attenuating to the value of σ_y, allowing greater amounts of energy to be absorbed plastically. This is exactly what an FGFM is designed to achieve: the yield stress σ_y of a graded foam diminishes in the *z*-direction as the density decreases. Ideally, in order to maximise the amount of plastic deformation in a graded foam, the yield stress σ_y at any point *z* should be equal to the stress wave magnitude σ_w at *z*, while the change in yield stress

between any two points z and $z+\delta z$ should be greater than $\delta\sigma_w$ over the distance δz. Symbolically:

$$\sigma_y \mid_z = \sigma_w \mid_z, \forall z \tag{4}$$

$$\frac{\partial \sigma_y}{\partial z} \geq \frac{\partial \sigma_w}{\partial z} \tag{5}$$

3.3 Conclusions

It has been shown that a FGFM can, under certain conditions, outperform traditional foams when employed as cushioning structures.

- It is shown that an FGFM can exhibit superior energy absorption over equivalent uniform foams under low energy impacts, and that convex perform better than concave gradients. This advantage is negated when the impact energy becomes significantly high such that low density regions of the graded foam become ineffective at bearing the higher load and densify after absorbing only a small fraction of the total energy. What constitutes a 'high energy impact' is somewhat difficult to define but depends on the average density of the foam and the density gradient.

- The variation in a cellular FGFM would make it extremely difficult to dynamically test and obtain valid results using a traditional SHPB apparatus, due to the limiting assumptions that are made for Equations (1) to (3). Variables that a FGM would introduce, such as a spatially varying yield stress, varying density and/or varying strain rate sensitivities, would almost certainly invalidate any efforts in ensuring stress-strain uniformity, in which case only an average stress-strain result could be obtained. This problem is overcome by virtually testing such materials since Equations (1) to (3) are not necessary to calculate the constitutive outputs.

- FGFMs are capable of reducing the duration of high accelerations during an impact event. This property could have wide implications in the head protection industry as many head injury criteria (e.g. HIC [15]) rely on acceleration durations as indicators of the likelihood for a person suffering significant head trauma. In this respect, protective headgear, e.g. safety helmets, employing FGFMs as the liner constituent may be advantageous to the wearer in reducing the risk of brain injury after a fall.

- Traditionally, many helmet certification standards (e.g. [16]) require a helmet to keep the acceleration of a headform dropped from a single drop height below some certain target level - achieving this is quite simple. However, recent helmet standards (e.g. [17]) demand that helmets be effective at multiple drop

heights, thus simulating both high and low energy impacts. This can be more difficult to achieve with current helmet liner technologies. FGFMs have been shown to exhibit significant advantages under low energy impact conditions while still performing nearly as well as their uniform counterpart under high energy conditions. These foams, carefully manufactured, may be one possible answer to the more stringent requirements of emerging helmet standards.

References

1. Hilyard, N.C., Djiauw, L.K. (1971) Observations on the Impact Behaviour of Polyurethane Foams; I. The Polymer Matrix. Journal of Cellular Plastics. 7:33–42
2. Mills, N.J., Gilchrist. (1991) The Effectiveness of Foams in Bicycle and Motorcycle Helmets. Accid. Anal. and Prev. 23:153–163
3. Di Landro, L., Sala, G., Olivieri, D. (2002) Deformation mechanisms and energy absorption of polystyrene foams for protective helmets. Polymer Testing 21:217–228
4. Avalle, M., Belingardi, G., Montanini. R., (2001) Characterization of polymeric structural foams under compressive impact by means of energy absorption diagram. International Journal of Impact Engineering 25:455–472
5. Al-Mousawi, M. M., Reid, S. R., Deans, W. F., (1997) The use of the split Hopkinson pressure bar techniques in high strain rate materials testing. Proc Instn Mech Engrs Part C 211:273–292
6. Bragov, A.M., Lomunov, A.K., Sergeichev, I.V., Tsembelis, K., Proud, W.G., (2008) Determination of physicomechanical properties of soft soils from medium to high strain rates. International Journal of Impact Engineering 35:967 - 976
7. Ninan, L., Tsai, J., Sun, C.T. (2001) Use of split Hopkinson pressure bar for testing off-axis composites. International Journal of Impact Engineering 25:291–313
8. Lee, O. S., Kim, M.S., (2004) Dynamic material property characterization by using split Hopkinson pressure bar (SHPB) technique. Nuclear Engineering and Design 226:119–125
9. Chen, W., Song, B., Frew, D. J., Forrestal, M. J., (2003) Dynamic Small Strain Measurements of a Metal Specimen with a Split Hopkinson Pressure Bar. Society for Experimental Mechanics 43:20–23
10. Miyamoto, Y, Kaysser, W.A., Rabin, B.H., Kawasaki, A., Ford, R.G., (1999) Functionally Graded Materials: Design, Processing and Applications. Materials Technology Series, Kluwer Academic Publishers
11. ABAQUS, ABAQUS Analysis User's Manual, Version 6.7, in: ©ABAQUS, Inc, 2007
12. Schraad, M. W., Harlow, F. H., (2006) A stochastic constitutive model for disordered cellular materials: Finite-strain uni-axial compression. International Journal of Solids and Structures 43:3542–3468
13. Zhao, H., Gary, G., (1995) A Three Dimensional Analytical Solution Of The Longitudinal Wave Propagation In An Infinite Linear Viscoelastic Cylindrical Bar. Application To Experimental Techniques. Journal of the Mechanics and Physics of Solids 43:1335–1348
14. Blanc, R. H., (1993) Transient Wave Propagation Methods for Determining the Viscoelastic Properties of Solids. Journal of Applied Mechanics 60:763–768
15. Newman, J. A., (1998) Kinematics of head injury - An overview, in: Frontiers in Head and Neck Trauma: Clinical and Biomechanical, IOS Press Inc., Burke, Virginia.
16. BSI, EN 1384: 1996 Specification for helmets for equestrian activities, in: London, British Standards Distribution, 1996
17. BSI, EN 14572:2005: High performance helmets for equestrian activities, in: London, British Standards Institution, 2005.